sustainability

MDPI

Article

Dense Forests in the Brazilian State of Amapá Store the Highest Biomass in the Amazon Basin

José Douglas M. da Costa [1], Paulo Eduardo Barni [2], Eleneide D. Sotta [3], Marcelo de J. V. Carim [4], Alan C. da Cunha [1], Marcelino C. Guedes [3], Perseu da S. Aparicio [5], Leidiane L. de Oliveira [6], Reinaldo I. Barbosa [7], Philip M. Fearnside [7], Henrique E. M. Nascimento [7] and José Julio de Toledo [1,8,*]

1 Graduate Program in Environmental Sciences, Federal University of Amapá UNIFAP, Macapá 68903-419, Brazil; jose.costa@ueap.edu.br (J.D.M.d.C.); alancunha12@gmail.com (A.C.d.C.)
2 Rorainópolis Campus, State University of Roraima UERR, Rorainópolis 69375-000, Brazil; paulinpa2007@gmail.com
3 Brazilian Agricultural Research Corporation EMBRAPA, Macapá 68903-197, Brazil; eleneide.sotta@embrapa.br (E.D.S.); marcelino.guedes@embrapa.br (M.C.G.)
4 Technology Development Coordination, Research Institute of Amapá State IEPA, Macapá 68903-419, Brazil; veigacarim@hotmail.com
5 Department of Forest Engineering, Amapá State University UEAP, Macapá 68900-070, Brazil; perseu.aparicio@ueap.edu.br
6 Institute of Water Science and Technology, Federal University of Western Pará UFOPA, Santarém 68040-255, Brazil; leidianeoli@gmail.com
7 Environmental Dynamics Coordination, National Institute for the Amazon Research INPA, Manaus 69067-375, Brazil; reinaldo@inpa.gov.br (R.I.B.); pmfearn@inpa.gov.br (P.M.F.); hnasci@gmail.com (H.E.M.N.)
8 Department of Environment and Development, Federal University of Amapá UNIFAP, Macapá 68903-419, Brazil
* Correspondence: jjulio@unifap.br; Tel.: +55-96-98146-9049

Abstract: The Amazonian forests located within the Guiana Shield store above-average levels of biomass per hectare. However, considerable uncertainty remains regarding carbon stocks in this region, mainly due to limited inventory data and the lack of spatial datasets that account for factors influencing variation among forest types. The present study investigates the spatial distribution of original total forest biomass in the state of Amapá, located in the northeastern Brazilian Amazon. Using data from forest inventory plots, we applied geostatistical interpolation techniques (kriging) combined with environmental variables to generate a high-resolution map of forest biomass distribution. The stocks of biomass were associated with different forest types and land uses. The average biomass was 536.5 ± 64.3 Mg ha^{-1} across forest types, and non-flooding lowland forest had the highest average (619.1 ± 38.3), followed by the submontane (521.8 ± 49.8) and the floodplain (447.6 ± 45.5) forests. Protected areas represented 84.1% of Amapá's total biomass stock, while 15.9% was in agriculture and ranching areas, but the average biomass is similar between land-use types. Sustainable-use reserves stock more biomass (40%) than integral-protection reserves (35%) due to the higher average biomass associated with well-structured forests and a greater density of large trees. The map generated in the present study contributes to a better understanding of carbon balance across multiple spatial scales and demonstrates that forests in this region contain the highest carbon stocks per hectare (260.2 ± 31.2 Mg ha^{-1}, assuming that 48.5% of biomass is carbon) in the Amazon. To conserve these stocks, it is necessary to go further than merely maintaining protected areas by strengthening the protection of reserves, restricting logging activities in sustainable-use areas, promoting strong enforcement against illegal deforestation, and supporting the implementation of REDD+ projects. These actions are critical for avoiding substantial carbon stock losses and for reducing greenhouse-gas emissions from this region.

check for updates

Academic Editor: Tim Gray

Received: 19 April 2025
Revised: 19 May 2025
Accepted: 26 May 2025
Published: 9 June 2025

Citation: da Costa, J.D.M.; Barni, P.E.; Sotta, E.D.; Carim, M.d.J.V.; da Cunha, A.C.; Guedes, M.C.; Aparicio, P.d.S.; de Oliveira, L.L.; Barbosa, R.I.; Fearnside, P.M.; et al. Dense Forests in the Brazilian State of Amapá Store the Highest Biomass in the Amazon Basin. *Sustainability* **2025**, *17*, 5310. https://doi.org/10.3390/su17125310

Keywords: Amazon Guiana Shield; biomass mapping; carbon stock; forest inventory; kriging; land-use change; geostatistics; greenhouse gases; protected areas; REDD+

1. Introduction

The Brazilian Amazon is one of the world's largest carbon reservoirs, storing around 59 Pg of carbon in biomass (live + dead, above + below ground) in addition to large amounts of carbon in the soil [1,2]. The Amazon forest plays an indispensable role in climate control and the global carbon balance [3]. However, the process of deforestation and hidden degradation (logging and understory fire) has resulted in a reduction in the forest's ability to absorb and store carbon [4]. The Amazon carbon sink was reduced by 30% over two decades (1990s–2000s), declining from 0.54 Pg yr^{-1} to 0.38 Pg yr^{-1} [5], while carbon stocks decreased by 18.3% over four decades (1970s–2010s), from 71.8 Pg to 58.6 Pg [2].

Biomass in Amazonian forests is studied by several groups of researchers and monitoring networks using atmospheric measurements. These include the LBA Data Model Intercomparison Project [6] and permanent plots such as those in the Amazonian Forest Inventory Network (RAINFOR) [7], the Amazonian Tree Diversity Network (ATDN) [8], and the Center for Tropical Forest Science—Forest Global Earth Observatory (CTFS-ForestGEO) network [9]. Biomass directly affects the calculation of carbon stocks, and biomass losses and gains affect emissions and uptakes of greenhouse gases [10–13].

Recent studies have highlighted the role of remote sensing tools in improving biomass mapping at high spatial resolution across the Amazon. Ref. [14] combined LiDAR, MODIS surface reflectance, and SRTM elevation data with inventory data from RADAMBRASIL project to generate detailed carbon maps. GEDI (Global Ecosystem Dynamics Investigation), based on spaceborne LiDAR, has enabled the estimation of carbon stocks and fluxes at both basin and regional scales with unprecedented spatial and temporal resolution [15,16]. Integrating airborne LiDAR, PALSAR radar, MODIS reflectance, and TRMM precipitation data, ref. [17], produced high-resolution biomass estimates across Amazonian forest types. Sentinel-2 spectral data have also been shown to accurately predict aboveground biomass in transitional forest–savanna ecotones [18]. Finally, ref. [19] showed that MODIS data, when combined with sparse LiDAR information, can provide high-resolution carbon density maps. These technological advances complement ground-based inventories and improve biomass estimation in remote or under-sampled forests of the Amazon.

Accurate estimates of the spatial distribution of forest biomass are necessary to reduce uncertainties in carbon stocks and greenhouse-gas emissions and to assist in reducing emissions from deforestation and forest degradation [4,20–23]. Advances in increasing the number of plots and their spatial scope in different ecosystems, as well as in improving inventories by increasing the accuracy of measurements and adding new variables (such as height and wood density) have been implemented in the last decades [24]. However, high intra- and inter-specific variation add spatial variability that needs to be studied and reduced to improve biomass estimates.

More accurate estimates of forest biomass can be achieved when spatial variability is taken into account. Environmental factors, such as soil, relief, and climate, can be used as predictors of the spatial distribution of forest biomass when there is a relationship between these variables and the different vegetation types [16,25–29]. Data from the forest inventories of the RADAMBRASIL project [30] conducted in the Brazilian Amazon have been used to determine the total biomass at 123.1 Pg (above- and belowground) [2,12]. Information on commercial volume is expanded to the total biomass (live + dead; below and aboveground) based on established expansion factors for different types of forests [1,2],

allowing the extrapolation of biomass in larger areas that encompass different types of forests [2,13,22,25–27,29,31].

The state of Amapá has data from inventories of vegetation in forest areas; however, systematic work has not yet been conducted to organize these data and assemble a map of the distribution of biomass and carbon. While much of the state's vegetation cover is still conserved, the increasing advance of illegal deforestation in forest areas will increase carbon emissions. Thus, determining the quantity and distribution of biomass and carbon in the different forest types in the state is essential for determining future losses in carbon stocks.

The general objective of this study was to model the spatial distribution of the dense ombrophilous forest biomass and to evaluate the total biomass stock (live + dead, above and belowground) in the state of Amapá. Our objectives were as follows: (i) to estimate the total forest biomass based on the expansion of the commercial volume of forest inventories carried out in dense ombrophilous forests in Amapá and surroundings; (ii) to produce a reference map through spatial modeling of forest biomass using geostatistical methods; (iii) to quantify the biomass density (Mg ha^{-1}) for each forest type and estimate the losses resulting from deforestation; and (iv) to estimate the original biomass stock in areas of agriculture and ranching use (settlement projects and other areas) and in protected areas (conservation units, indigenous lands, and *quilombola* areas). Brazil's "conservation units" are areas protected for biodiversity and "*quilombola*" areas are protected for the descendants of escaped African slaves, who are traditional peoples with the same rights as indigenous peoples under Brazil's 1988 constitution.

2. Materials and Methods

2.1. Study Area

The state of Amapá is located in the northeastern portion of the Brazilian Amazon and has an area of 142.8 × 10^3 km^2 (Figure 1). Intact forest covers 97% of the state, with 73% corresponding to protected areas, including conservation units and indigenous and *quilombola* lands [32–34].

The climate is humid tropical monsoon, with a minimum temperature of 26 °C and maximum of 33 °C [35–38]. The northern and coastal regions of the state have higher annual rainfall that varies between 2700 and 2900 mm, whereas in other parts of the state precipitation varies between 2300 and 2700 mm in the southern portion and between 2000 and 2200 mm in the west and southwest (Tumucumaque Mountains and Jari River areas) [37,39,40].

The vegetation in Amapá is characterized by the predominance of dense ombrophilous forest (75.5%), which is classified into four forest types: (i) dense-canopy rainforest on river floodplain (Da), (ii) dense-canopy rainforest on non-flooding lowlands (Db), (iii) dense-canopy rainforest, submontane (Ds), and (iv) dense-canopy rainforest, montane (Dm) [41,42] (Figure 1 and Table 1).

Table 1. Forest types and their respective areas in the state of Amapá.

Forest Type	Vegetation Code [a]	Dense Ombrophilous Forest	
		Area (10^3 km^2)	Area (%)
Dense-canopy rainforest on river floodplain	Da	6.07	4.3
Dense-canopy rainforest on non-flooding lowlands	Db	20.71	14.5
Dense-canopy montane rainforest	Dm	0.4	0.3
Dense-canopy submontane rainforest	Ds	80.58	56.4
Total		107.76	75.5

[a] Vegetation codes [35]. Areas are for the year 2018.

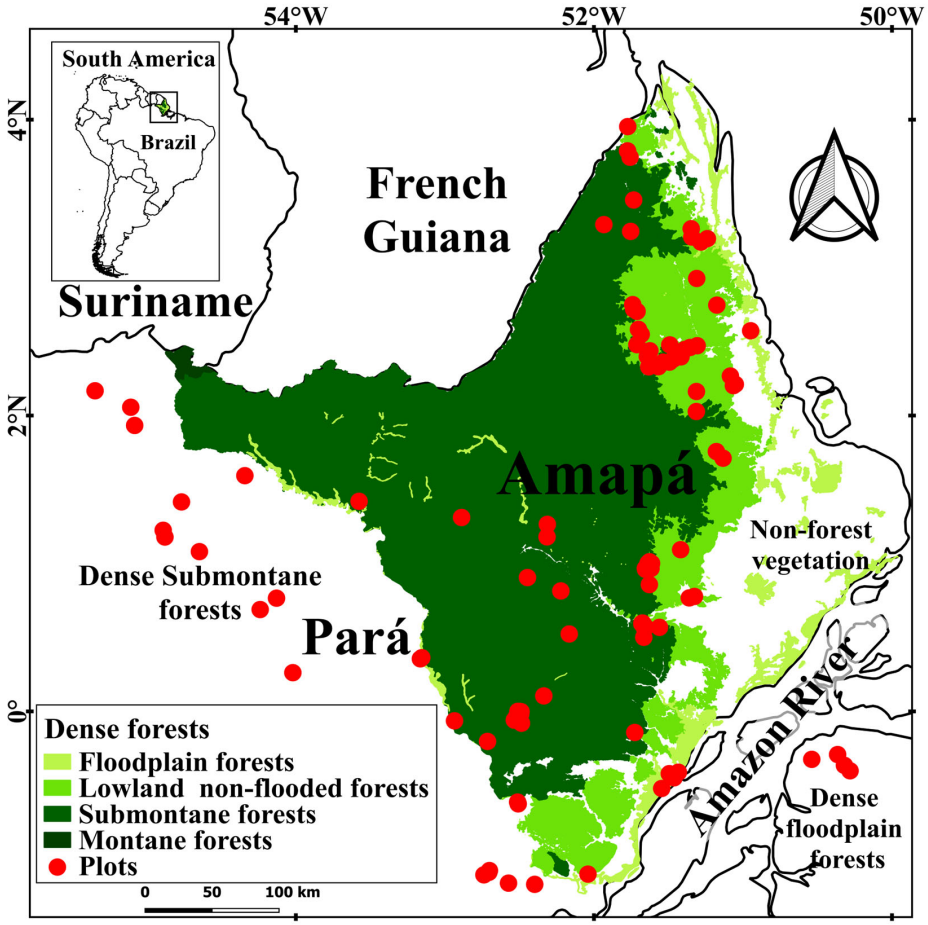

Figure 1. Spatial allocation of forest inventory plots across distinct forest types within the state of Amapá and extending up to 100 km beyond its borders. The forest areas represent those still standing in 2018.

In river floodplains the predominant soil is alluvial with medium to high fertility, with a flooding period that is associated with the effect of the daily tides, and during the rainy season many areas remain flooded or at least the soils are saturated with water [39,40]. The main botanical families are Fabaceae, Arecaceae, Clusiaceae, Malvaceae, Myrtaceae, and Mimosaceae [43–45].

In non-flooding lowland forests, the predominant soils are red-yellow latosol and yellow latosol (Ultisols) [46,47], and the relief varies considerably (elevations between 5 m and 100 m), with areas that are quite flat and dissected by a network of streams that undergo periodic flooding during the rainy season. The Sapotaceae, Lecythidaceae, Fabaceae, Burseraceae and Chrysobalanaceae families are predominant [48].

In submontane forests, the predominant soil is red-yellow latosol [46,47], with a gently undulating to hilly relief and elevations of 100 m, rarely exceeding 500 m. This vegetation type is characterized by primary communities with little or no change and has some trees exceeding 60 m in height. The families Meliaceae, Annonaceae, Chrysobalanaceae, Sapotaceae, Burseraceae, Euphorbiaceae, Lauraceae, Myrtaceae, and Lecythidaceae are the most abundant [45].

In the montane forests the predominant soil is red-yellow latosol [46,47]. The relief is mountainous, and the Tumucumaque mountains stands out in the westernmost part of the state near the triple border between Brazil, French Guiana, and Suriname with a topography of rocky outcrops and hills with altitudes of 600 m to 700 m [42,49].

2.2. Boundaries of Dense Ombrophilous Forest Types

The definition of the limits of the dense ombrophilous forest in Amapá were derived from a vegetation map of the Environmental Information Database (BDIA) at a scale of 1:250,000 [41]. The dense ombrophilous forest is divided into four forest types, but the montane forest (Dm) type is excluded due to the absence of forest inventories in the area and because it occupies a very small area (0.3%). The three remaining forest types were used for this study: river floodplain (Da), non-flooding lowlands (Db), and submontane forest (Ds) (Table 1).

2.3. Biomass Estimation

The estimation of the total original biomass (live and dead, above and belowground) per unit area (Mg ha^{-1}) was performed using data from 129 plots: 15 plots in the river floodplain, 59 in the non-flooding lowlands, and 55 in the submontane forest (Figures 1 and 2). Of these, 54 1 ha plots (100 × 100 m) were from the RADAMBRASIL forest inventories [30]: 37 plots located in the state of Amapá (3 plots in the river floodplain, 21 in the non-flooding lowlands, and 13 in the submontane forest); 17 plots in the surrounding region (state of Pará) within 100 km of the state border (4 plots in the river floodplain, 1 in the non-flooding lowlands, and 12 in the submontane forest) [42]. From these inventories, we used information on the commercial volume of trees with circumference at breast height—CBH ≥ 100 cm (diameter at breast height—DBH ≥ 31.8 cm) measured 1.3 m above the ground or above any buttresses. To this database, were added 75 plots of more recent inventories in Amapá, with 8 plots in the river floodplain, 37 in the non-flooding lowlands, and 30 in the submontane forest. These included 4 types of forest inventory plots: 33 square plots (100 × 100 m) and 13 rectangular plots (40 × 250 m), each measuring 1 ha; 8 transect plots (0.5 ha each), consisting of 20 subplots (10 × 125 m) distributed along 1 km transects; and 21 clustered plots (8 ha each), composed of 20 subplots (20 × 200 m) arranged in 5 crosses, with 4 subplots per cross. In these plots, only individuals with a DBH ≥ 31.8 cm were used for biomass calculations, in order to minimize the variability between recent inventories and those of the RADAMBRASIL project.

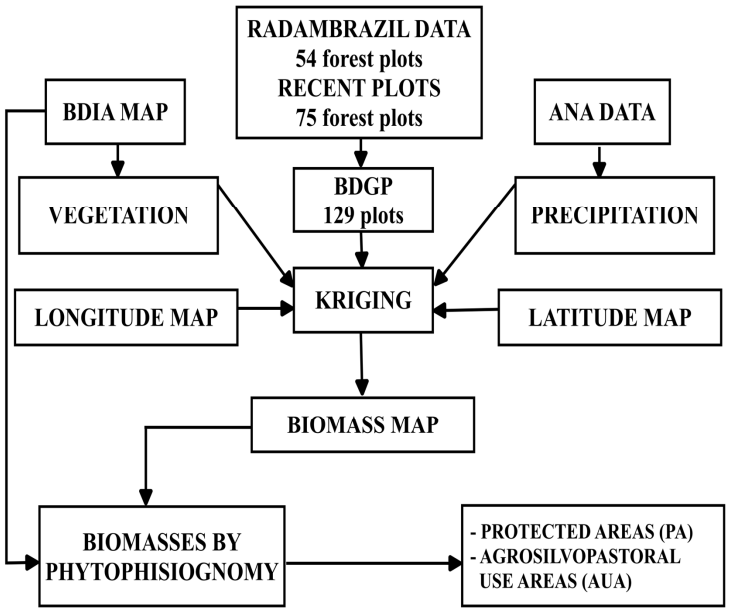

Figure 2. Flowchart illustrating the methodological steps for estimating forest biomass in the state of Amapá. BDIA = Environmental Information Database. BDGP = database of georeferenced plots. ANA = National Water Agency.

The bole volume (V_b) up to the height (H_b) of the first thick branch of each of the 19,544 inventoried trees, was calculated using the following equation [34]:

$$V_b = \frac{[\pi \times D^2]}{[4 \times H_b \times 0.7]} \quad (1)$$

where π is equal to 3.1416 and D is the tree DBH. An adjustment factor of 0.956 was applied to the resulting bole volume to correct for hollow and irregularly shaped trees [1]. In cases where bole height measurements were unavailable, we fitted site-specific allometric models using a sample of DBH and bole height data available for each location (Supplementary Material: Table S1). Then, the wood density (wood specific gravity as kiln dry weight divided by the green volume; g cm^3) obtained in the Global Wood Density Database through the taxonomic identity of the trees [50] was used for each tree. When there was no identification at the species level, the average for the genus or family was used, and when there was no identification, the average of the plot was used. The bole volume and basic wood density of each tree were transformed at the plot level (in 1 ha) to apply the expansion factors, which were applied to all 129 sampling plots to convert bole volume (m^3 ha^{-1}) into total biomass (Mg ha^{-1}).

The volume expansion factor (*VEF*) is the volume ratio [1] given by dividing the bole volume estimated for all trees $\geq$ 10 cm DBH by the volume estimated for trees with DBH $\geq$ 31.8 cm. Therefore, the *VEF* adjusted the volume to represent the trees with DBH between 10 cm and 31.8 cm, which are not included in the RADAMBRASIL forest surveys. The *VEF* value used was 1.537, normalized according to the expected diameter distribution for dense forests of Central Amazon [1]. This means that the volume of trees with DBH between 10 and 31.8 cm corresponds to 53.7% of the volume of trees with DBH $\geq$ 31.8 cm.

The biomass expansion factor (*BEF*) is a biomass ratio obtained by the division of total aboveground biomass of the trees by the bole biomass [1]. Thus, the *BEF* was adjusted for the crown biomass of the trees normalized by the diameter distribution of dense forests of central Amazon [1]. The bole biomass was multiplied by the *BEF*, whose value was 1.635 if the bole biomass was $\geq$190 Mg ha^{-1} (calculated by [1] from data by [51]), meaning that crown biomass is 63.5% of the bole biomass of the tree. The equation below was used if the biomass of the bole was <190 Mg ha^{-1}, assuming the crown biomass varied depending on bole biomass:

$$BEF = exp[3.213 - 0.506 \times \ln(B_b)] \quad (2)$$

where *exp* is the antilogarithm, *ln* is the natural logarithm (base ~2.72), and B_b is the bole biomass.

To transform the values of expanded biomass into total biomass, we applied specific expansion factors representing the contribution of each component relative to aboveground living biomass as follows: 0.065 for trees < 10 cm DBH [51]; 0.019 for palms, 0.034 for vines, 0.043 for seedlings [1]; and 0.0021 for other non-tree forest components [12,52]. The aboveground dead biomass was estimated using expansion factors of 0.094 for coarse wood debris (both fallen and standing) and 0.041 for fine litter. The below-ground biomass was estimated by applying a factor of 0.31 [1].

2.4. Validation and Determination of the Interpolation Model

The georeferenced dataset was randomly split into two subsets: one comprising 116 sampling plots (~90%), and the other comprising 13 plots (~10%). The largest subset (N = 116) was used to develop the spatial models, while the smaller subset (N = 13) was set aside for model validation and for selecting the most accurate interpolation model following the generation of forest biomass maps.

2.5. Criteria for Validation and Model Selection

In order to validate and select the most suitable interpolation model, the following criteria were applied [53]: (i) the smallest mean square error (MSE), (ii) the greatest efficiency percentage (%EF), and (iii) the highest adjusted coefficient of determination (R^2). Both the MSE and %EF were used as measures of accuracy, while the adjusted R^2 served as an indicator of precision [54]. The adjusted R^2 was also used to assess model precision, expressed as a percentage error: $(\varepsilon) = (1 - R^2) \times 100$.

The parameters were calculated from the 13-point subsample. These values were then compared with the predictions generated by the three interpolation models (ordinary kriging, co-kriging, and kriging with external drift) at the same geographic coordinates [27,55,56].

2.6. Modeling and Spatial Distribution of Biomass

The spatial distribution of forest biomass was determined based on the best model among the three kriging techniques [27] (Figure 3): (i) ordinary kriging, (ii) co-kriging, and (iii) kriging with external drift (KED). Kriging was performed in ArcGIS software, version 10.7 (Esri, Redlands, CA, USA, 2019), and consisted of estimating values of a spatial variable in non-sampled locations and assessing the uncertainty associated with the predicted value [24,54]. To perform kriging, first a semivariogram must be modeled. The semivariogram function quantifies the assumption that nearby points tend to be more similar than more distant points and illustrates the spatial dependence among the sample plots [24,27,54,57]. Once the distances between all pairs of plots are plotted, a model is then fitted to the resulting data. To accomplish this, the semivariogram relies on three key components [53,54]: (i) the "nugget", which reflects the data's variability at very short distances, often indicating measurement error or a lack of spatial continuity; (ii) the "sill", representing the level at which the semivariance stabilizes and the values no longer increase with distance; and (iii) the "range", which defines the maximum distance over which spatial correlation exists, beyond which the samples are considered to be uncorrelated. A conceptual model for calculating the semivariogram (SV) is given as follows:

$$SV = N + (S + N) \times R \quad (3)$$

where N is the nugget effect, S is the sill, and R is the range.

For ordinary kriging, the semivariogram was modeled with the sample point variable (total biomass) as an input, thus obtaining a continuous biomass map for the predicted values (Mg ha^{-1}) from known data [53]. In the co-kriging analysis, along with the primary variable (total biomass), three auxiliary variables were incorporated, including (i) the vegetation map (V) from the BDIA database, which classifies the area into three forest types, (ii) the annual average precipitation map (P), obtained from the website of the National Water Agency [39], and (iii) the longitude map (Lo) produced from the longitude of each known point. The three maps were designed for UTM/Zone 22 N, WGS 84, and transformed into a raster format with a spatial resolution of one hectare per pixel.

For KED, the final biomass map (Mg ha^{-1}) was obtained by applying multiple linear regression using the raster maps (cell grid) of the auxiliary variables V, P, latitude (La), Lo, and R (map of residuals) as independent variables. The KED map was created in three stages: (1) obtaining the residuals and the regression coefficients by applying the least squares method between the main variable and the auxiliary variables (sample points), (2) obtaining the raster map of residuals (1 ha spatial resolution, UTM/Zone 22 N, and WGS 84) through ordinary waste kriging, and (3) execution of the multiple linear regression as follows:

$$KED_B = 1481.43611 - 7.913882 \times R + 7.748431 \times V + 0.060044 \times P - 16.401831 \times La + 23.73743 \times Lo \quad (4)$$

where KED_B is the total biomass obtained by kriging with external drift, *R* is the map of residuals, *V* is the vegetation map, *P* is the precipitation map, *La* is the latitude map, and *Lo* is the longitude map. The model explained 84% of the variability in KED biomass, and all coefficients contributed significantly to the model ($P = 0.03$ for *La*, and $P < 0.001$ for the other parameters).

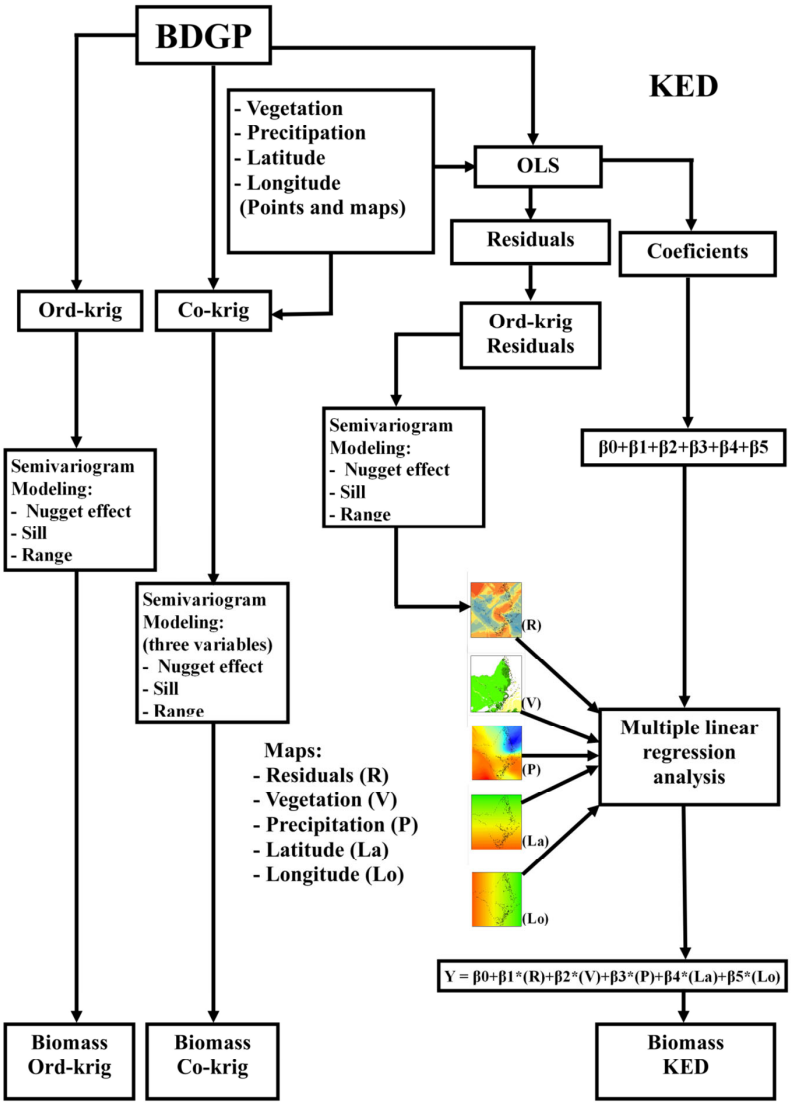

Figure 3. Flowchart illustrating the application of kriging to the georeferenced database, incorporating five auxiliary environmental variables. BDGP = database of georeferenced plots; OLS = ordinary least squares; R = map of residuals; V = vegetation map; P = precipitation map; La = latitude map; Lo = longitude map; Ord-krig = ordinary kriging; Co-krig = co-kriging; KED = kriging with external drift. For co-kriging, three auxiliary variables were employed (V, P, and Lo), and for KED, five variables were utilized (R, V, P, La, and Lo). The colors in the small maps represent the gradients of R, V, P, La, and Lo, ranging from lower values (yellowish to reddish tones) to higher values (greenish to bluish tones).

2.7. Biomass Maps for Forest Types

In order to estimate the biomass associated with each forest type, binary raster maps (values 0 and 1) with a spatial resolution of one hectare were generated on the BDIA classification. In these maps, pixels corresponding to the extension of a given forest type were assigned the value 1, while all other areas were assigned the value 0. Each raster was constructed with identical dimensions: 6153 rows by 5392 columns. These binary layers were then individually overlaid with the dense forest biomass map (Mg ha^{-1}) through

map-algebra procedures, resulting in biomass distribution maps for each forest type, as shown in the following equation:

$$B_{ft(i)} = M_{t(i)} \times M_{dfB} \quad (5)$$

where: $B_{ft(i)}$ is the biomass map for the forest type "*i*", $M_{t(i)}$ is the map of class "*i*" generated from the BDIA map (Da, Db, and Ds), and M_{dfB} refers to the dense forest biomass maps.

2.8. Biomass in Protected Areas and Agriculture and Ranching Areas

To determine the biomass in protected areas, cross-referencing between the binary maps of conservation units, indigenous lands, and *quilombola* areas was applied using databases from the Ministry of the Environment [58] and the National Institute for Colonization and Agrarian Reform (INCRA) [59], with the biomass maps generated by forest type. The biomasses of the agriculture and ranching use areas (settlement projects and other areas) were determined by excluding the protected areas. Conservation units were divided into "integral-protection" units (which aim to preserve nature and allow only indirect use of their natural resources), and "sustainable-use" units (which aim to combine nature conservation with sustainable use of part of their natural resources).

2.9. Statistical Analysis

The Shapiro–Wilk normality test was applied to all datasets obtained by cross-referencing information between the land-use categories. The *t*-test was used to determine whether the values predicted by the three models (ordinary kriging, co-kriging, and kriging with external drift) and the values of the subsample had different means [49]. These analyses were run using R software, version 3.5.1 (R Development Core Team, Vienna, Austria, 2018). The multiple regression was used to predict the values of the final map produced in ArcGIS software by kriging with external drift using maps of the auxiliary variables (vegetation, precipitation, latitude, longitude, and residuals).

3. Results

The model with the best performance in representing the total biomass of the dense ombrophilous forest in the state of Amapá was KED (Figure 4 and Table 2). The final fitted semivariogram (exponential structure) had a range of 168 km and a strong spatial correlation of the data, with a nugget effect of 8% in relation to the threshold (20,141 m). Nevertheless, the spatial correlation declined, with spatial dependence dropping between 168 km and 253 km, beyond which, the relationships between the samples became random.

Table 2. Cross-validation results (accuracy) and selection of the optimal interpolation model for estimating the mean total biomass of dense ombrophilous forest in the state of Amapá. MSE = mean square error; %EF = efficiency percentage; adjusted R^2 = adjusted coefficient of determination; BDGP = georeferenced database; Ord-krig = ordinary kriging; Co-krig = co-kriging; KED = kriging with external drift.

Interpolators	MSE	%EF	Adjusted R^2	*p*-Value Regression	*p*-Value *t*-Test	Mean Biomass (Mg ha^{-1})
BDGP (13 plots)	-	-	-	-	-	594.01
Ord-krig	126.9	96.70	0.48	0.0052	0.057	524.81
Co-krig	123.4	93.19	0.45	0.0069	0.071	531.47
KED	121.7	83.04	0.61	0.0010	0.092	534.78

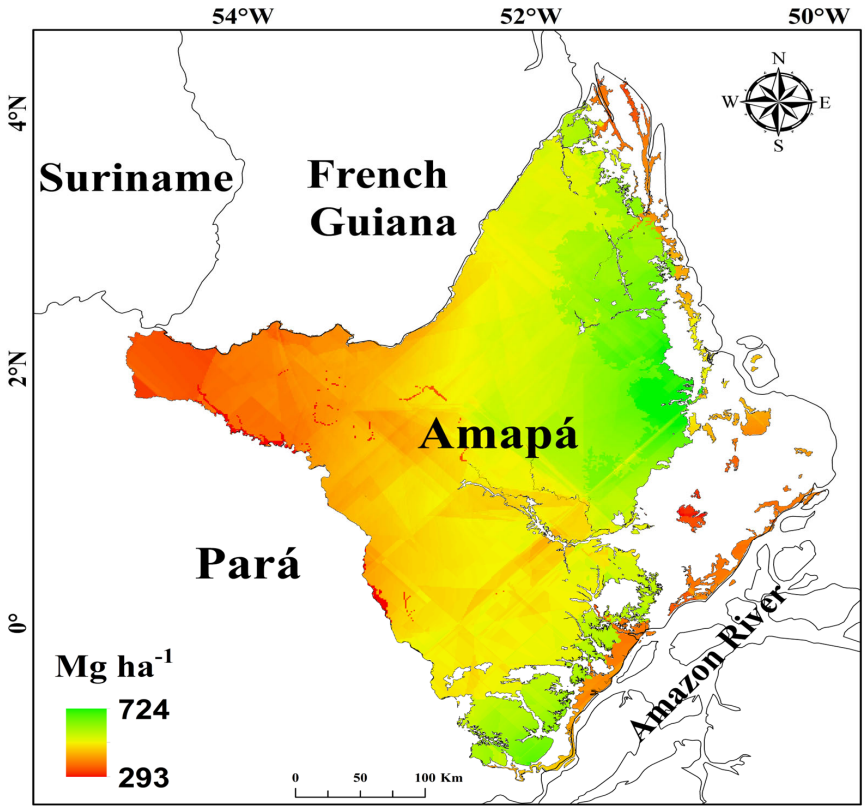

Figure 4. Reference map showing the spatial distribution of forest biomass (Mg ha^{-1}) in the state of Amapá, generated using kriging with external drift (KED). White areas represent non-forest vegetation.

The average biomass across forest types in the state of Amapá was 536.5 ± 64.3 Mg ha^{-1} (Table 3; Figure 4), corresponding to 260.2 ± 31.2 Mg C ha^{-1}, assuming that 48.5% of biomass is carbon [22]. Non-flooding lowland forest was the forest type that had the highest average total biomass (619.13 ± 38.27 Mg ha^{-1}; mean ± SD), followed by the submontane forest (521.83 ± 49.82 Mg ha^{-1}) and the floodplain forest, which had the lowest mean (447.60 ± 45.51 Mg ha^{-1}). The total biomass stock (live + dead, above and belowground) for the dense ombrophilous forest in the state of Amapá (still standing in 2018) using the KED model was estimated at 5.66 × 10^9 Mg for 107,193 km^2 (71.9% of the state's territory). Of this total, live aboveground biomass accounted for 4.10 × 10^9 Mg (72.4%), dead aboveground biomass accounted for 0.65 × 10^9 Mg (11.5%), and live belowground biomass accounted for 0.91 × 10^9 Mg (16.1%) (Table 3). The cumulative loss of biomass by 2018 in Amapá due to deforestation was 0.098 × 10^9 Mg (1.74%) (Table 3). The lowland rain forest had the highest cumulative loss (0.056 × 10^9 Mg; 0.99%).

Table 3. Original total biomass stock (live + dead; above- and belowground) and estimated weighted average per unit area for dense ombrophilous forest in the state of Amapá, representing biomass losses due to deforestation.

Forest Type	Area (10^3 km^2)	Live Above-ground (10^9 Mg) [b]	Dead Above-ground (10^9 Mg) [b]	Live Below-ground (10^9 Mg) [b]	Total Biomass Stock (10^9 Mg)	Bio. Stock (%)	Mean (±SD) (Mg ha^{-1})	Range (Mg ha^{-1})	Biomass Loss (10^9 Mg)	Bio. Loss (%)
Da [a]	6.051	0.174	0.028	0.039	0.241	4.3	447.60 ± 45.51	293.0–692.0	0.008	0.14
Db [a]	20.688	0.895	0.143	0.199	1.237	21.9	619.13 ± 38.27	397.0–724.0	0.056	0.99
Ds [a]	80.454	3.026	0.484	0.672	4.182	73.9	521.83 ± 49.82	293.0–709.0	0.033	0.58
Total	107.193	4.096	0.655	0.909	5.659	100.0	536.48 ± 64.25	293.0–724.0	0.098	1.73

[a] Vegetation codes [35]. Data are for the year 2018. [b] The proportions used for calculation of biomass by forest compartment were produced following ref. [22].

The total amount of biomass stored within protected areas (conservation units, indigenous lands, and *quilombola* areas) in Amapá, was estimated at 4.76 × 10^9 Mg (84.13%; 535.08 ± 64.67 Mg ha^{-1}) (Table 4). The largest stock was in conservation units (75%; 4.24 × 10^9 Mg), with 58.78% (3.32 × 10^9 Mg) in submontane forest, 14.65% (0.829 × 10^9 Mg) in non-flooding lowland rainforest, and only 1.56% (0.088 × 10^9 Mg) in river floodplain forest. The total stock in areas of agriculture and ranching use was 0.898 × 10^9 Mg (15.87%; 532.15 ± 61.26 Mg ha^{-1}), and settlement projects had the largest stock (9.18%; 0.519 × 10^9 Mg), with the most biomass in the submontane forest type (5.87%; 0.332 × 10^9 Mg).

Table 4. Area (km^2), average biomass (Mg ha^{-1}; %), range of biomass values (Mg ha^{-1}), biomass stock (Mg), and biomass losses (10^6 Mg; %) due to deforestation up to 2018, by forest type and land-use group in the state of Amapá.

Group	Area (10^3 km^2)	Mean (±SD) (Mg ha^{-1})	Range (Mg ha^{-1})	Biomass Stock (10^6 Mg)	Bio. Stock (%)	Biomass Loss (10^6 Mg)	Bio. Loss (%)
Protected areas							
Indigenous lands							
Dense-canopy rainforest on river floodplain	0.21	434.16 ± 22.58	348–600	9.24	0.16	0.01	0.11
Dense-canopy rainforest on non-flooding lowlands	1.20	601.24 ± 10.87	547–622	72.39	1.28	1.21	1.67
Dense-canopy rainforest, submontane	8.16	511.10 ± 34.96	348–612	416.89	7.37	3.18	0.76
Total in indigenous lands	9.57	515.50 ± 46.13	348–622	498.52	8.81	4.40	0.88
Conservation units							
Dense-canopy rainforest on river floodplain	2.03	435.00 ± 53.62	293–655	88.45	1.56	0.07	0.08
Dense-canopy rainforest on non-flooding lowlands	13.24	626.08 ± 35.74	397–721	829.06	14.65	13.94	1.68
Dense-canopy rainforest, submontane	63.78	521.58 ± 53.64	293–709	3326.44	58.78	7.74	0.23
Total in conservation units	79.05	537.55 ± 66.28	293–721	4243.95	75.00	21.75	0.51
Quilombola areas							
Dense-canopy rainforest on river floodplain	0.02	427.46 ± 9.31	415–438	1.01	0.02	0.04	3.96
Dense-canopy rainforest on non-flooding lowlands	0.29	611.26 ± 8.50	581–641	17.43	0.31	0.02	0.11
Dense-canopy rainforest, submontane	-	-	-	-	-	-	
Total in quilombola areas	0.31	519.36 ±49.66	415–641	18.44	0.33	0.06	0.33
Total in protected areas	88.93	535.08 ± 64.67	293–721	4760.91	84.13	26.21	0.55
Agriculture and ranching areas							
Settlement projects							
Dense-canopy rainforest on river floodplain	0.56	460.01 ± 34.44	398–618	25.74	0.45	1.77	6.88
Dense-canopy rainforest on non-flooding lowlands	2.64	610.47 ± 36.90	425–722	161.29	2.85	19.01	11.79
Dense-canopy rainforest, submontane	6.21	535.42 ± 17.14	412–671	332.41	5.87	14.86	4.47
Total in settlement projects	9.41	535.30 ± 51.03	398–722	519.43	9.18	35.65	6.86

Table 4. *Cont.*

Group	Area (10^3 km^2)	Mean (±SD) (Mg ha^{-1})	Range (Mg ha^{-1})	Biomass Stock (10^6 Mg)	Bio. Stock (%)	Biomass Loss (10^6 Mg)	Bio. Loss (%)
Other areas							
Dense-canopy rainforest on river floodplain	3.22	453.42 ± 38.36	312–692	109.52	1.94	6.58	6.01
Dense-canopy rainforest on non-flooding lowlands	3.32	602.44 ± 47.01	397–724	168.50	2.98	22.29	13.23
Dense-canopy rainforest, submontane	2.31	531.12 ± 25.09	619–654	100.37	1.77	7.74	7.71
Total in other areas	8.85	529.00 ± 73.33	312–724	378.39	6.69	36.61	9.68
Total in agriculture and ranching areas	18.26	532.15 ± 61.26	312–724	897.82	15.87	72.25	8.05
Grand total	107.19	536.48 ± 64.25	293–724	5658.73	100.00	98.47	1.74

The agriculture and ranching areas had the highest cumulative losses of biomass in the total stock of Amapá (72.25 × 10^6 Mg; 8.05%; Table 4). The protected areas had the lowest cumulative losses (26.21 × 10^6 Mg; 0.55%).

Conservation units maintain the largest area of submontane forest cover in the state of Amapá, stocking a substantial amount of biomass. The total biomass stock in sustainable-use conservation units was estimated at 2263.30 × 10^6 Mg (572.79 ± 56.24 Mg ha^{-1}), 40% of the total, while that in the integral-protection conservation units was lower, 1980.62 × 10^6 Mg (502.27 ± 55.90 Mg ha^{-1}), or 35% of the total (Table 5). The largest stock was in the Tumucumaque Mountains National Park (an integral-protection conservation unit), estimated at 1872.98 × 10^6 Mg (500.91 ± 54.74 Mg ha^{-1}), followed by the Amapá State Forest (a sustainable-use conservation unit), estimated at 1325.85 × 10^6 Mg (588.10 ± 55.10 Mg ha^{-1}). Amapá National Forest had the highest average biomass stock for sustainable-use units (599 ± 29.32 Mg ha^{-1}), while the highest for integral-protection units was for the Jari Ecological Station (533.55 ± 6.28 Mg ha^{-1}).

Table 5. Area (km^2), biomass stock (Mg; %), average biomass (Mg ha $^{-1}$), and biomass range (Mg ha^{-1}) in 2018 for conservation units in the state of Amapá.

Conservation Unit	Area (10^3 km^2)	Biomass Stock (10^6 Mg)	Biomass Stock (%)	Mean (±SD) (Mg ha^{-1})	Range (Mg ha^{-1})
Integral Protection					
Tumucumaque Mountains National Park	37.29	1872.98	33.1	500.91 ± 54.74	293–613
Cabo Orange National Park	1.37	71.73	1.3	524.07 ± 84.45	394–639
Jari Ecological Station	0.67	35.91	0.6	533.55 ± 6.28	515–552
Total in integral-protection units	39.34	1980.62	35.0	502.27 ± 55.90	293–639
Sustainable Use					
Amapá State Forest	22.80	1325.85	23.4	588.10 ± 55.10	397–721
Cajari River Extractive Reserve	3.71	215.81	3.8	580.52 ± 47.62	443–658
Amapá National Forest	4.50	274.92	4.9	599.00 ± 29.32	495–654
Iratapuru River Sustainable Development Reserve	8.70	446.73	7.9	513.66 ± 23.62	340–552
Total in sustainable-use units	39.71	2263.30	40.0	572.79 ± 56.24	340–721
Total in conservation units	79.05	4243.93	75.0	537.23 ± 66.28	293–721

Biomass distribution using estimates for each pixel showed asymmetrical patterns for the different land-use types (Figure 5A), which are related to distinct peaks of biomass frequency for different forest types (Figure 5B). Agriculture and ranching areas had a higher frequency of pixels with low biomasses (400–460 Mg ha^{-1}), which coincide with

a peak of frequency for forests on river floodplain. The highest frequency for integral-protection conservation units (450–520 Mg ha^{-1}) matches the high frequency for sub-montane forests (500–550 Mg ha^{-1}) and the high frequency of pixels with large biomass stocks (500–600 Mg ha^{-1}) for sustainable-use conservation units overlapped with peaks of frequency for both submontane and lowland forests (550–620 Mg ha^{-1}).

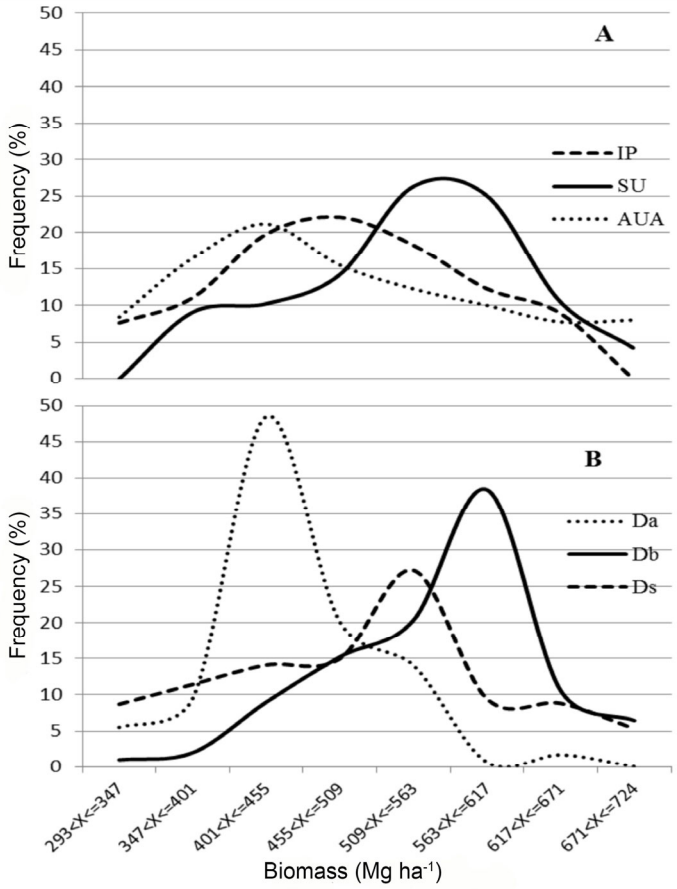

Figure 5. Biomass (Mg ha^{-1}) distribution (frequency of pixels expressed as percentage) (**A**) across conservation units and areas used for agriculture and ranching, and (**B**) by forest type. IP = integral-protection conservation units; SU = sustainable-use conservation units; AUA = agriculture and ranching use areas; Da = dense-canopy rainforest on river floodplain; Db = dense-canopy rainforest on non-flooding lowlands; Ds = dense-canopy rainforest, submontane.

4. Discussion

We fitted total biomass data from a geographic database of forest inventories [41] and mapped it using kriging with external drift to generate an improved modeling of stocks of forest biomass for Amapá. The semivariogram revealed that 84% of the variation in total biomass is spatially structured, with spatial dependence extending up to 168 km across the study area. Approaches based on simple average per forest type are less effective for mapping biomass than geostatistical methods, which account for spatial correlations among sampling plots [27,31,60]. Despite the robustness of the approach, this study has some weaknesses that should be addressed in future research. A key limitation is the absence of a temporal analysis of biomass change over the past 5 to 10 years, which would enable a better understanding of trends in carbon dynamics across the region. The lack of temporal consistency between data from plots inventoried in the 1970s by the RADAMBRASIL project and those from more recent inventories (2000s–2010s) may increase uncertainty in the spatial modeling of current biomass. Additionally, the absence of field data in some areas, particularly in remote regions of western Amapá such as

the Tumucumaque Mountains National Park, has constrained spatial interpolation and increased model uncertainty. Future research should focus on incorporating time-series remote sensing data from LiDAR or GEDI missions [21–24,27] and expanding ground-truth inventories in under-sampled regions to improve both the temporal and spatial resolution of biomass estimates.

An important feature of this research was the relatively high plot density of one plot per 835 km^2. This plot density is higher than that for the forest inventories in the state of Roraima (1480 km^2) [27] and for the RADAMBRASIL Project for the forest area of the Brazilian Amazon as a whole (one plot per 2702 km^2). This higher density indicates an improvement in the spatial analysis of the total biomass data by forest type, with a high spatial resolution of 1 ha, thereby decreasing the uncertainty as compared to other research on the Amazon that has spatial resolution of 1 km^2 [13,22,27].

The use of interpolation techniques incorporating environmental variables (latitude, longitude, precipitation, vegetation type, and residuals) produced significant results in multiple linear regression, explaining a large portion of the variability (84%) in the interpolated biomass. Longitude, precipitation and vegetation showed positive relationships with biomass; that is, the larger the values of these variables, the greater the forest biomass. This increase in biomass with longitude reflects a gradient toward the eastern region of Amapá, where precipitation is higher and lowland non-flooded forests are prevalent (see Figure 1), supporting greater biomass stocks. The positive effect of precipitation is expected, as water availability enhances photosynthesis, tree growth, and forest productivity, thereby promoting biomass accumulation [61]. In addition, forest types with greater structural complexity, such as lowland non-flooded and submontane forests of the northeastern Amazon, typically store more biomass due to the higher density of large trees [62,63]. Nonetheless, the contribution of a database of georeferenced forest inventories from French Guiana [64] and the western portion of Amapá would enhance the accuracy of biomass models, since the absence of data in these surrounding regions was the primary source of error (39%) in the spatial modeling. However, the present reference map produced in this study (Figure 4) offers a reliable representation of the spatial distribution of total forest biomass in Amapá.

Regarding average forest biomass per hectare, the findings revealed that the modeled estimates (537 Mg ha^{-1}) in Amapá may exceed those of the broader Brazilian Amazon by 75% to 124% depending on the reference estimate (307 Mg ha^{-1} to 240 Mg ha^{-1}) [1,17]. Particularly, the Guiana Shield is known to store high amounts of biomass (370–434 Mg ha^{-1}) [1,28], but the small sample size (27 plots for [28] and 37 for [1]) indicates uncertainty in the estimates and in the capacity for extrapolation to large areas of forest in this region. All of the forest types in Amapá had higher averages in our study than those reported in the Brazilian Amazon as a whole [1]. The average in non-flooding lowland rainforest was the one with the highest difference (60% higher) in relation to the average for the Amazon, while submontane and river-floodplain forests were 35% and 24% higher [1].

The higher biomass density observed in Amapá's forests, compared to other regions of the Brazilian Amazon, can be attributed to a combination of ecological, biogeographic, and methodological factors. Amapá lies within the Guiana Shield, a region characterized by well-preserved, structurally complex forests with a high density of large, long-lived tree species and lower historical disturbance levels [62]. These forests often contain a higher proportion of large (DBH > 30 cm) and tall trees (reaching over 70 m in height; [64]). For instance, large trees in lowland forests of the Amapá National Forest have an average height of 32 m [65], whereas trees of similar diameter typically reach lower heights in the dense forests of the southwestern (24 m) and central (27 m) Amazon [66]. Dominant large-tree species in the region, such as *Dinizia excelsa*, *Manilkara* spp., and *Vouacapoua americana*, are

characterized by high wood density, which contributes substantially to the aboveground biomass in Amapá's forests [28,29]. Additionally, the climatic conditions in Amapá, marked by relatively high precipitation and minimal dry season stress, favor continuous forest productivity, a higher density of large trees, and greater biomass accumulation [29,61,63]. Furthermore, past studies in the region have relied on limited sample sizes, especially in remote or upland areas, which may have led to underestimates of biomass [1,17]. In contrast, the present study includes a larger and more spatially representative dataset, improving the accuracy of biomass estimates and better capturing the contribution of high-biomass forest types prevalent in Amapá.

In the present study, montane dense forest was excluded due to limited inventory data. However, future studies could address this gap using remote sensing tools such as LiDAR, GEDI, or Sentinel-2 imagery [18,67]. These technologies can provide reliable biomass estimates in remote areas and improve the completeness of forest carbon assessments across different tropical forest types. However, this study used a dataset combining past with recent inventories and applied a reliable methodology to improve the spatial distribution of the biomass estimates. The results show that forest areas in Amapá store more biomass than previously reported.

The total biomass of the protected areas was estimated at 4760.91 $\times$ 10^6 Mg, representing 84.1% of the total biomass of Amapá. These estimates indicate that the protected areas in Amapá are strategic for mitigating losses of carbon stocks and for reducing greenhouse-gas emissions, and these areas form part of a large set of protected areas in the Amazon that are essential for maintaining carbon stocks [23,68–70]. These protected areas play an important role in mitigating the effects of global climate change and may represent future opportunities for the state of Amapá under REDD+ projects. These projects have the potential to reduce greenhouse-gas emissions [70] and benefit the traditional populations that live in them through commitments to maintain the forest standing [70–72].

The largest stock observed in protected areas was in the conservation units (75% of total). The sustainable-use conservation units contributed 40% of the total biomass stock, while integral-protection reserves contributed 35% due to differences in average biomass. The higher biomass in the sustainable-use reserves is due to differences in biomass per unit area (14% higher in the sustainable-use areas), since both types of conservation unit occupy similar areas (37.0% for sustainable-use vs. 36.7% for integral-protection reserves).

In Amapá National Forest, a total stock of 274.92 $\times$ 10^6 Mg was estimated, which is 56% higher than that estimated for this conservation unit by [73], who reported a total of 176.47 $\times$ 10^6 Mg of biomass. The largest stock was in Tumucumaque Mountains National Park, estimated at 1872.98 $\times$ 10^6 Mg, which is 26% higher than the estimate of 1482.50 $\times$ 10^6 Mg by [73]. For Amapá State Forest, 1325.85 $\times$ 10^6 Mg was estimated, which is 49% higher than the 891.56 $\times$ 10^6 Mg estimated by [73]. Since the methods used to estimate plot biomass in [69] and in the present study were the same, the observed differences are likely due to the inclusion of a greater number of sample plots from recent inventories in the Amapá National Forest (13 plots) and in the Amapá State Forest (32 plots). These additions likely contributed to increased estimation accuracy for these two protected areas. Although no new plots were added in the Tumucumaque Mountains National Park, the plots from the other two reserves included submontane forests, which represent the most common forest type across these protected areas. Furthermore, the previous study [69] relied on biomass maps from [1], which were based solely on RADAMBRASIL plots. Because those plots were mostly located near rivers, they likely failed to adequately sample large tree species such as *Dinizia excelsa* and *Manilkara* spp., which are common on the region's plateaus [63]. In contrast, our study incorporated different environmental predictors (precipitation, longitude, and latitude) which helped improve the precision of

biomass spatialization in areas lacking sample plots, resulting in more accurate estimates for these protected areas.

Protected areas play an important role in preventing emissions from deforestation [74]. The biomass stocks (and consequently, the carbon stock) currently held in protected areas are at less risk of being emitted into the atmosphere by deforestation than the carbon stored in vegetation located outside of protected areas. In addition to their value for conservation of biological diversity, protected areas are valuable because they have large amounts of carbon. This carbon is especially valuable because it is in areas that are under legal protection, although these areas have varying levels of access and permitted use of natural resources. Amapá State Forest and Amapá National Forest together contribute 28% of the biomass stock in the State of Amapá, and both reserves are under concession for selective logging. Because timber extraction focuses mainly on large trees with dense wood, the negative impacts will be higher on biomass stocks and consequently on carbon stocks, thus constraining the capacity of the protected areas to mitigate greenhouse-gas emissions. To conserve these stocks, it is therefore necessary to go further than simply maintaining protected areas; the uses permitted in sustainable-use protected areas must be rethought since most forest biomass is stored in conservation units where logging is currently allowed and is actively promoted by the government.

Since sustainable-use reserves hold a substantial portion of Amapá's carbon stocks, policy changes are urgently needed to guarantee their long-term carbon storage services. Strong regulation and, most recommended, the cessation of industrial logging concessions in sustainable-use reserves are required [75]. Further, it is necessary to implement zero-deforestation supply chains, such as afforestation on degraded lands for wood supply, as well as to support community-based forest management that aligns conservation goals with local livelihoods such as the productive chains from essential oils of *Carapa guianensis*, *Pentaclethra macroloba*, and *Copaifera* spp. [76–78]. Expansion of REDD+ initiatives and payments for ecosystem services [70] can also contribute to making forest conservation economically viable for local populations. Without such changes in public policy, the carbon storage of Amapá's forests could be drastically reduced, and both local and global climate potential could be compromised.

5. Conclusions

Advances have been made in the quantification of stocks and in mapping the spatial distribution of the total forest biomass in the state of Amapá, thereby helping to minimize uncertainties related to the spatial variation of forest biomass. The present study highlights the need for mapping the spatial distribution of forest biomass stocks using a larger number of plots in surrounding areas to minimize local uncertainties regarding carbon reservoirs.

The map generated here has high spatial resolution and provides valuable information for determining the carbon balance at multiple scales, offering further evidence that Amapá's forests contain the largest per-hectare biomass stocks in the Brazilian Amazon.

These stocks are concentrated in protected areas, mainly sustainable-use reserves. Changes to public policies regarding these protected areas are needed to prevent the depletion of carbon stocks and mitigate the emission of greenhouse gases. Therefore, it is crucial to promote public policies that strengthen the protection of reserves, the implementation of effective enforcement to reduce deforestation to zero, and the cessation of logging activities in sustainable-use areas. Additionally, supporting community-based forest management, such as productive chains from essential oils, and mechanisms such as REDD+ and payment for ecosystem services can enhance the effectiveness of protected areas, ensuring the conservation of carbon stocks in the region.

Supplementary Materials: The following supporting information can be downloaded at: https://www.mdpi.com/article/10.3390/su17125310/s1, Table S1. Local allometric models using diameter at breast height (DBH) to estimate bole height (H_b).

Author Contributions: Conceptualization, J.J.d.T. and P.E.B.; methodology, J.D.M.d.C., P.E.B. and J.J.d.T.; formal analysis, J.D.M.d.C. and P.E.B.; investigation, J.D.M.d.C., P.E.B., E.D.S., M.d.J.V.C., A.C.d.C., M.C.G., P.d.S.A. and L.L.d.O.; data curation, E.D.S., M.d.J.V.C., A.C.d.C., M.C.G., P.d.S.A., L.L.d.O., R.I.B. and P.M.F.; writing—original draft preparation, J.D.M.d.C., P.E.B. and J.J.d.T.; writing—review and editing, P.E.B., E.D.S., M.d.J.V.C., A.C.d.C., M.C.G., P.d.S.A., L.L.d.O., R.I.B., P.M.F., H.E.M.N. and J.J.d.T.; visualization, H.E.M.N.; supervision, P.E.B. and J.J.d.T. All authors have read and agreed to the published version of the manuscript.

Funding: This research was funded by the National Council for Scientific and Technological Development (CNPq): Universal (#409827/2021-5 and #459735/2014-4) and Pro-Amazonia (#444350/2024-1). J.J.deT. was supported by CNPq with a Research Productivity Scholarship (#316281/2021-2). The article processing charge was funded by the Federal University of Amapá (UNIFAP) and its Vice-Rectorate for Research and Graduate Studies (PROPESPG; Call for applications #01/2024). P.M.F. thanks the CNPq (#312450/2021-4 and #406941/2022-0), FAPEAM (#01.02.016301.02529/2024-87), and the Brazilian Research Network on Climate Change (FINEP/Rede Clima #01.13.0353-00). A.C.da C. was supported by CNPq with a Research Productivity Scholarship (#314830/2021-9).

Institutional Review Board Statement: Not applicable.

Informed Consent Statement: Not applicable.

Data Availability Statement: The data presented in this study are available upon request from the corresponding author.

Conflicts of Interest: Eleneide D. Sotta and Marcelino C. Guedes were employed by Brazilian Agricultural Research Corporation EMBRAPA. The remaining authors declare that the research was conducted in the absence of any commercial or financial relationships that could be construed as a potential conflict of interest.

References

1. Nogueira, E.M.; Fearnside, P.M.; Nelson, B.W.; Barbosa, R.I.; Keizer, E.W.H. Estimates of forest biomass in the Brazilian Amazon: New allometric equations and adjustments to biomass from wood-volume inventories. *For. Ecol. Manag.* **2008**, *256*, 1853–1867. [CrossRef]
2. Nogueira, E.M.; Yanai, A.M.; Fonseca, F.O.R.; Fearnside, P.M. Carbon stock loss from deforestation through 2013 in Brazilian Amazonia. *Glob. Chang. Biol.* **2015**, *21*, 1271–1292. [CrossRef]
3. Flores, B.M.; Montoya, E.; Sakschewski, B.; Nascimento, N.; Staal, A.; Betts, R.A.; Levis, C.; Lapola, D.M.; Esquível-Muelbert, A.; Jakovac, C.; et al. Critical Transitions in the Amazon Forest System. *Nature* **2024**, *626*, 555–564. [CrossRef]
4. Qin, Y.; Xiao, X.; Wigneron, J.-P.; Ciais, P.; Brandt, M.; Fan, L.; Li, X.; Crowell, S.; Wu, X.; Doughty, R.; et al. Carbon loss from forest degradation exceeds that from deforestation in the Brazilian Amazon. *Nat. Clim. Chang.* **2021**, *11*, 442–448. [CrossRef]
5. Brienen, R.J.W.; Phillips, O.L.; Feldpausch, T.R.; Gloor, E.; Baker, T.R.; Lloyd, J.; Lopez-Gonzalez, G.; Monteagudo-Mendoza, A.; Malhi, Y.; Lewis, S.L.; et al. Long-Term Decline of the Amazon Carbon Sink. *Nature* **2015**, *519*, 344–348. [CrossRef] [PubMed]
6. de Gonçalves, L.G.G.; Borak, J.S.; Costa, M.H.; Saleska, S.R.; Baker, I.; Restrepo-Coupe, N.; Muza, M.N.; Poulter, B.; Verbeeck, H.; Fisher, J.B.; et al. Overview of the large-scale biosphere–atmosphere experiment in Amazonia data model intercomparison project (lba dmip). *Agric. For. Meteorol.* **2013**, *182*, 111–127. [CrossRef]
7. Blundo, C.; Carilla, J.; Grau, R.; Malizia, A.; Malizia, L.; Osinaga-Acosta, O.; Bird, M.; Bradford, M.; Catchpole, D.; Ford, A.; et al. Taking the pulse of Earth's tropical forests using networks of highly distributed plots. *Biol. Conserv.* **2021**, *260*, 108849.
8. Ter Steege, H.; de Oliveira, S.M.; Pitman, N.C.A.; Sabatier, D.; Antonelli, A.; Guevara Andino, J.E.; Aymard, G.A.; Salomão, R.P. Towards a dynamic list of Amazonian tree species. *Sci. Rep.* **2019**, *9*, 3501. [CrossRef]
9. Anderson-Teixeira, K.J.; Davies, S.J.; Bennett, A.C.; Gonzalez-Akre, E.B.; Muller-Landau, H.C.; Wright, S.J.; Abu Salim, K.; Almeyda Zambrano, A.M.; Alonso, A.; Baltzer, J.L.; et al. CTFS-ForestGEO: A worldwide network monitoring forests in an era of global change. *Glob. Chang. Biol.* **2015**, *21*, 528–549. [CrossRef]
10. Chave, J.; Condit, R.; Aguilar, S.; Hernandez, A.; Lao, S.; Perez, R. Error propagation and scaling for tropical forest biomass estimates. *Philos. Trans. R. Soc. B* **2024**, *359*, 409–420. [CrossRef]

11. Chave, J.; Réjou-Méchain, M.; Búrquez, A.; Chidumayo, E.; Colgan, M.S.; Delitti, W.B.C.; Duque, A.; Eid, T.; Fearnside, P.M.; Goodman, R.C.; et al. Improved allometric models to estimate the aboveground biomass of tropical trees. *Glob. Chang. Biol.* **2014**, *2*, 3177–3190. [CrossRef] [PubMed]
12. Fearnside, P.M. Global warming and tropical land-use change: Greenhouse gas emissions from biomass burning, decomposition and soils in forest conversion, shifting cultivation and secondary vegetation. *Clim. Chang.* **2000**, *46*, 115–158. [CrossRef]
13. Houghton, R.A. How well do we know the flux of CO_2 from land-use change? *Tellus B Chem. Phys. Meteorol.* **2010**, *62*, 337–351. [CrossRef]
14. Englund, O.; Sparovek, G.; Berndes, G.; Freitas, F.; Ometto, J.P.; Oliveira, P.V.C.; Costa, C., Jr.; Lapola, D. A new high-resolution nationwide aboveground carbon map for Brazil. *Geo Geogr. Environ.* **2017**, *4*, e00045. [CrossRef]
15. Mamani, N.; Finer, M.; Ariñez, A.; Amazon carbon update, based on NASA's GEDI mission. MAAP 2022, Report #199. Available online: https://maaproject.kinsta.cloud/?html2pdf=https://www.maapprogram.org/maap-199-amazon-carbon-update-based-on-nasas-gedi-mission/&media=print (accessed on 13 May 2025).
16. Dionizio, E.A.; Giannini, T.C.; Gastauer, M.; Barbosa-Silva, R.G.; de Souza, R.L.F.; Nunes, S.; Ramos, S.J.; Andrino, C.O.; Cavalcante, R.B.L. Aboveground carbon stocks for different forest types in eastern Amazonia. *Environ. Res. Commun.* **2025**, *7*, 045006. [CrossRef]
17. Ometto, J.P.; Gorgens, E.B.; de Souza Pereira, F.R.; Sato, L.; de Assis, M.L.R.; Cantinho, R.; Longo, M.; Jacon, A.D.; Keller, M. A biomass map of the Brazilian Amazon from multisource remote sensing. *Sci. Data* **2023**, *10*, 668. [CrossRef] [PubMed]
18. Faria, L.D.d.; Matricardi, E.A.T.; Marimon, B.S.; Miguel, E.P.; Junior, B.H.M.; Oliveira, E.A.d.; Prestes, N.C.C.d.S.; Carvalho, O.L.F.d. Biomass prediction using sentinel-2 imagery and an artificial neural network in the Amazon/Cerrado transition tegion. *Forests* **2024**, *15*, 1599. [CrossRef]
19. Jiang, X.; Li, G.; Lu, D.; Moran, E.; Batistella, M. Modeling Forest Aboveground Carbon Density in the Brazilian Amazon with Integration of MODIS and Airborne LiDAR Data. *Remote Sens.* **2020**, *12*, 3330. [CrossRef]
20. Harris, N.L.; Brown, S.; Hagen, S.C.; Saatchi, S.S.; Petrova, S.; Salas, W.; Hansen, M.C.; Potapov, P.V.; Lotsch, A. Baseline map of carbon emissions from deforestation in tropical regions. *Science* **2012**, *336*, 1573–1576. [CrossRef] [PubMed]
21. Nepstad, D.C.; McGrath, D.G.; Soares-Filho, B. Systemic conservation, REDD, and the future of the Amazon Basin. *Conserv. Biol.* **2011**, *25*, 1113–1116. [CrossRef]
22. Saatchi, S.S.; Harris, N.L.; Brown, S.; Lefsky, M.; Mitchard, E.T.A.; Salas, W.; Zutta, B.R.; Buermann, W.; Lewis, S.L.; Hagen, S.; et al. Benchmark map of forest carbon stocks in tropical regions across three continents. *Proc. Nat. Acad. Sci. USA* **2011**, *108*, 9899–9904. [CrossRef] [PubMed]
23. Soares-Filho, B.; Moutinho, P.; Nepstad, D.; Anderson, A.; Rodrigues, H.; Garcia, R.; Dietzsch, L.; Merry, F.; Bowman, M.; Hissa, L.; et al. Role of Brazilian Amazon protected areas in climate change mitigation. *Proc. Nat. Acad. Sci. USA* **2010**, *107*, 10821–10826. [CrossRef]
24. Sullivan, M.J.P.; Lewis, S.L.; Hubau, W.; Qie, L.; Baker, T.R.; Banin, L.F.; Chave, J.; Cuni-Sanchez, A.; Feldpausch, T.R.; Lopez-Gonzalez, G.; et al. Field methods for sampling tree height for tropical forest biomass estimation. *Methods Ecol. Evol.* **2018**, *9*, 1179–1189. [CrossRef]
25. Campos, M.S.; Anjos, L.J.S.; de Souza, E.B.; Bezerra, F.G.S.; de Lima, A.M.M.; Galbraith, D.R.; Adami, M. Prioritizing Amazon Forest Conservation: Assessing Potential Biomass under Climate Change. *Glob. Ecol. Conserv.* **2024**, *54*, e03106. [CrossRef]
26. Baccini, A.; Goetz, S.J.; Walker, W.S.; Laporte, N.T.; Sun, M.; Sulla-Menashe, D.; Hackler, J.; Beck, P.S.A.; Dubayah, R.; Friedl, M.A.; et al. Estimated carbon dioxide emissions from tropical deforestation improved by carbon-density maps. *Nat. Clim. Chang.* **2012**, *2*, 182–185. [CrossRef]
27. Barni, P.E.; Manzi, A.O.; Condé, T.M.; Barbosa, R.I.; Fearnside, P.M. Spatial distribution of forest biomass in Brazil's state of Roraima, northern Amazonia. *For. Ecol. Manag.* **2016**, *377*, 170–181. [CrossRef]
28. Feldpausch, T.R.; Lloyd, J.; Lewis, S.L.; Brienen, R.J.W.; Gloor, M.; Monteagudo, A.; Lopez-Gonzalez, G.; Banin, L.; Kamariah, A.S.; Affum-Baffoe, K.; et al. Tree height integrated into pantropical forest biomass estimates. *Biogeosciences* **2012**, *9*, 3381–3403. [CrossRef]
29. Malhi, Y.; Wood, D.; Baker, T.R.; Wright, J.; Phillips, O.L.; Cochrane, T.; Meir, P.; Chave, J.; Almeida, S.; Arroyo, L.; et al. The regional variation of aboveground live biomass in old-growth Amazonian forests. *Glob. Chang. Biol.* **2006**, *12*, 1107–1138. [CrossRef]
30. Brazil, RADAMBRASIL. *Levantamento dos Recursos Naturais (Folhas SA.22 Macapá)*; Ministério das Minas e Energia: Rio de Janeiro, RJ, Brazil, 1973–1983.
31. Sales, M.H.; Souza, C.M., Jr.; Kyriakidis, P.C.; Roberts, D.A.; Vidal, E. Improving spatial distribution estimation of forest biomass with geostatistics: A case study for Rondônia, Brazil. *Ecol. Model.* **2007**, *205*, 221–230. [CrossRef]
32. Brazil, MCT (Ministério da Ciência e Tecnologia). *Segunda Comunicação Nacional do Brasil À Convenção-Quadro das Nações Unidas Sobre Mudança do Clima*; MCT: Brasília, DF, Brazil, 2010; p. 280.

33. Brazil, Secretaria de Estado do Meio Ambiente—Amapá. *Relatório Técnico de Desmatamento No Estado do Amapá, Referente Ao príodo 2013 E 2014*; SEMA-AP: Macapá, AP, Brazil, 2015; p. 32.
34. Brazil, Secretaria de Estado do Meio Ambiente—Amapá. *Relatório Técnico de Desmatamento No Estado do Amapá, Referente Ao Período 2015 E 2016*; SEMA-AP: Macapá, AP, Brazil, 2017; p. 6.
35. Drummond, J.A.; Dias, T.C.A.C.; Brito, D.M.C. *Atlas das Unidades de Conservação do Estado do Amapá*; Secretaria de Estado do Meio Ambiente—Amapá: Macapá, AP, Brazil, 2008.
36. Alvares, C.A.; Stape, J.L.; Sentelhas, P.C.; Gonçalves, J.L.; Sparovek, G. Koppen's climate classification map for Brazil. *Meteorol. Z.* **2013**, *22*, 711–728. [CrossRef]
37. Brazil, INMET (Instituto Nacional de Meteorologia), Normal Climatológica do Brasil. Available online: https://portal.inmet.gov.br/normais (accessed on 10 December 2018).
38. Peel, M.C.; Finlayson, B.L.; McMahon, T.A. Updated World Map of the Köppen-Geiger Climate Classification. *Hydrol. Earth Syst. Sci.* **2007**, *11*, 1633–1644. [CrossRef]
39. Brazil, ANA (Agência Nacional de Águas), Precipitação Média Annual—Série de 1977 A 2006. Available online: http://dadosabertos.ana.gov.br/datasets/ (accessed on 23 July 2018).
40. Souza, E.B.; Cunha, A.C. Climatologia de precipitação no Amapá e mecanismos climáticos de grande escala. In *Tempo, Clima E Recursos Hídricos–Resultados do Projeto REMETAP No Amapá*; Cunha, A.C., Souza, E.B., Cunha, H.F.A., Eds.; IEPA: Macapá, AP, Brazil, 2010; Volume 10, pp. 177–195.
41. Brazil, BDIA (Banco de Dados de Informações Ambientais), Mapa de Vegetação. Available online: https://bdiaweb.ibge.gov.br/#/consulta/vegetacao/ (accessed on 24 July 2018).
42. Brazil, IBGE (Instituto Brasileiro de Geografia e Estatística). *Manual Técnico da Vegetação Brasileira—Manuais Técnicos em Geociências*, 2nd ed.; IBGE: Rio de Janeiro, Brazil, 2012; p. 271.
43. Almeida, S.; Silva, M.S.; Rosa, N.A. Análise fitossociológica e uso de recursos vegetais na Reserva Extrativista do Cajari, Amapá. *Bol. Do Mus. Para. Emilio Goeldi* **1996**, *11*, 61–74.
44. Carim, M.J.V.; Jardim, M.A.G.; Medeiros, T.D.S. Composição florística e estrutura de floresta de várzea no município de Mazagão, Estado do Amapá, Brasil. *Sci. For.* **2008**, *36*, 191–201.
45. Costa-Neto, S.V.; Silva, M.S. *Projeto Zoneamento Ecológico-Econômico do Setor Costeiro Estuarino do Estado do Amapá: Diagnóstico Sócio-Ambiental, Relatório Técnico de Vegetação*; Governo do Amapá: Macapá, Brazil, 2023; p. 38.
46. Brazil, BDIA (Banco de Dados de Informações Ambientais), Mapa de Pedologia. Available online: https://bdiaweb.ibge.gov.br/#/consulta/pedologia/ (accessed on 27 October 2018).
47. Peres, R.N.; Serruya, N.M.; Vieira, L.S. Levantamento Exploratório de Solos. In *Brazil, Projeto RADAM-BRASIL. Folha NA/NB.22 Macapá. Levantamento de Recursos Naturais*; Departamento Nacional de Produção Mineral: Rio de Janeiro, RJ, Brazil, 1974; Volume 6.
48. Brazil, INAM (Instituto Natureza Amazônica). *Relatório do Inventário Florestal Amostral da Floresta Estadual do Amapá*; Brazil, INAM: Macapá, AP, Brazil, 2010; p. 176.
49. Brazil, ICMBIO (Instituto Chico Mendes de Conservação da Biodiversidade). *Plano de Manejo do Parque Nacional Montanhas do Tumucumaque*; Brazil, ICMBIO: Brasília, DF, Brazil, 2009. Available online: https://www.gov.br/icmbio/pt-br/assuntos/biodiversidade/unidade-de-conservacao/unidades-de-biomas/amazonia/lista-de-ucs/parna-montanhas-do-tumucumaque/arquivos/parna_montanhasdotumucumaque.pdf (accessed on 19 October 2018).
50. Zanne, A.E.; Lopez-Gonzalez, G.; Coomes, D.A.; Ilic, J.; Jansen, S.; Lewis, S.L.; Miller, R.B.; Swenson, N.G.; Wiemann, M.C.; Chave, J. Data from: Towards a worldwide wood economics spectrum [Dataset]. *Dryad* 2009. Available online: https://datadryad.org/dataset/doi:10.5061/dryad.234 (accessed on 11 October 2018).
51. Higuchi, N.; Santos, J.; Ribeiro, R.J.; Minette, L.; Biot, Y. Biomassa da parte aérea da vegetação de floresta tropical úmida de terra-firme da Amazônia Brasileira. *Acta Amaz.* **1988**, *28*, 153–165. [CrossRef]
52. Castilho, C.V.; Magnusson, W.E.; de Araújo, R.N.O.; Luizão, R.C.C.; Luizão, F.J.; Lima, A.P.; Higuchi, N. Variation in aboveground tree live biomass in a central Amazonian Forest: Effects of soil and topography. *For. Ecol. Manag.* **2006**, *234*, 85–96. [CrossRef]
53. Isaaks, E.; Srivastava, R. *Applied Geostatistics*; Oxford University Press: New York, NY, USA, 1989.
54. Landim, P.M.B.; Sturaro, J.R. Krigagem Indicativa Aplicada À Elaboração de Mapas Probabilísticos de Riscos. Available online: https://www.researchgate.net/profile/Jose-Sturaro-2/publication/251884208_KRIGAGEM_INDICATIVA_APLICADA_A_ELABORACAO_DE_MAPAS_PROBABILISTICOS_DE_RISCOS/links/55f8266f08ae07629dd0cce8/KRIGAGEM-INDICATIVA-APLICADA-A-ELABORACAO-DE-MAPAS-PROBABILISTICOS-DE-RISCOS.pdf (accessed on 10 April 2018).
55. Bello-Pineda, J.; Hernándes-Stefanoni, J.L. Comparing the performance of two spatial interpolation methods for creating a digital bathymetric model of the Yucatan submerged platform. *Pan-Am. J. Aquat. Sci.* **2007**, *2*, 247–254.
56. Gardiman Junior, B.S.; Magalhães, I.A.L.; Freitas, C.A.A.; Cecílio, R.A. Análise de técnicas de interpolação para espacialização da precipitação pluvial na bacia do rio Itapemirim (ES). *Ambiência* **2012**, *8*, 61–71. [CrossRef]

57. Barni, P.E.; Barbosa, R.I.; Xaud, H.A.M.; Xaud, M.R.; Fearnside, P.M. Precipitation in northern Amazonia: Spatial distribution in Brazil's State of Roraima. *Soc. Nat.* **2020**, *32*, 439–456. [CrossRef]
58. Brasil, MMA (Ministério do Meio Ambiente), Dados Georreferenciados das Unidades de Conservação. Available online: https://www.gov.br/icmbio/pt-br/assuntos/dados_geoespaciais/mapa-tematico-e-dados-geoestatisticos-das-unidades-de-conservacao-federais (accessed on 8 October 2018).
59. Brasil, INCRA (Instituto Nacional de Colonização E Reforma Agrária), Acervo Fundiário. Available online: https://acervofundiario.incra.gov.br/acervo/login.php (accessed on 10 November 2018).
60. Morais, V.A.; Santos, C.A.; Mello, J.M.; Dadid, H.C.; Araújo, E.J.G.A.; Scolforo, J.R.S. Spatial and vertical distribution of litter and belowground carbon in a Brazilian cerrado vegetation. *Cerne* **2017**, *23*, 43–52. [CrossRef]
61. Muller-Landau, H.C.; Cushman, K.C.; Arroyo, E.E.; Martinez Cano, I.; Anderson-Teixeira, K.J.; Backiel, B. Patterns and Mechanisms of Spatial Variation in Tropical Forest Productivity, Woody Residence Time, and Biomass. *New Phytol.* **2021**, *229*, 3065–3087. [CrossRef]
62. Slik, J.W.F.; Paoli, G.; McGuire, K.; Amaral, I.; Barroso, J.; Bastian, M.; Blanc, L.; Bongers, F.; Boundja, P.; Clark, C.; et al. Large trees drive forest aboveground biomass variation in moist lowland forests across the tropics. *Glob. Ecol. Biogeogr.* **2013**, *22*, 1261–1271. [CrossRef]
63. Gorgens, E.B.; Nunes, M.H.; Jackson, T.; Coomes, D.; Keller, M.; Reis, C.R.; Valbuena, R.; Rosette, J.; de Almeida, D.R.A.; Gimenez, B.; et al. Resource availability and disturbance shape maximum tree height across the Amazon. *Glob. Chang. Biol.* **2021**, *27*, 177–189. [CrossRef] [PubMed]
64. Chave, J.; Riéra, B.; Dubois, M.A. Estimation of biomass in a neotropical forest of French Guiana: Spatial and temporal variability. *J. Trop. Ecol.* **2001**, *17*, 79–96. [CrossRef]
65. Baia, A.L.P.; Nascimento, H.E.M.; Guedes, M.C.; Hilário, R.R.; Toledo, J.J. Tree height-diameter allometry and implications for biomass estimates in Northeastern Amazonian forests. *PeerJ* **2025**, *13*, e18974. [CrossRef]
66. Nogueira, E.M.; Nelson, B.W.; Fearnside, P.M.; França, M.B.; Oliveira, A.C.A. Tree height in Brazil's 'arc of deforestation': Shorter trees in south and southwest Amazonia imply lower biomass. *For. Ecol. Manag.* **2008**, *255*, 2963–2972. [CrossRef]
67. Dubayah, R.; Blair, J.B.; Goetz, S.; Fatoyinbo, L.; Hansen, M.; Healey, S.; Hofton, M.; Hurtt, G.; Kellner, J.; Luthcke, S.; et al. The global ecosystem dynamics investigation: High-resolution laser ranging of the Earth's forests and topography. *Sci. Remote Sens.* **2020**, *1*, 100002. [CrossRef]
68. Nepstad, D.C.; Veríssimo, A.; Alencar, A.; Nobre, C.; Lima, E.; Lefebvre, P.; Schlesinger, P.; Potter, C.; Moutinho, P.; Mendoza, E.; et al. Largescale impoverishment of Amazonian forests by logging and fire. *Nature* **1999**, *398*, 505–508. [CrossRef]
69. Pfaff, A.; Robalino, J.; Herrera, D.; Sandoval, C. Protected areas' impacts on Brazilian Amazon deforestation: Examining conservation-development interactions to inform planning. *PLoS ONE* **2015**, *10*, e0129460. [CrossRef]
70. Bousfield, C.G.; Massam, M.R.; Peres, C.A.; Edwards, D.P. Carbon payments can cost-effectively improve logging sustainability in the Amazon. *J. Environ. Manag.* **2022**, *314*, 115094. [CrossRef]
71. Greenleaf, M. The value of the untenured forest: Land rights, green labor, and forest carbon in the Brazilian Amazon. *J. Peasant Stud.* **2019**, *47*, 286–305. [CrossRef]
72. Yanai, A.M.; Fearnside, P.M.; Graça, P.M.L.A.; Nogueira, E.M. Avoided deforestation in Brazilian Amazonia: Simulating the effect of the Juma Sustainable Development Reserve. *For. Ecol. Manag.* **2012**, *282*, 78–91. [CrossRef]
73. Nogueira, E.M.; Yanai, A.M.; Vasconcelos, S.S.; Graça, P.M.L.A.; Fearnside, P.M. Carbon stocks and losses to deforestation in protected areas in Brazilian Amazonia. *Reg. Environ. Chang.* **2018**, *18*, 261–270. [CrossRef]
74. Cantinho, R.Z.; Linares, J.A.H.; Vieira, J.L.; Bustamante, M.M.C. Protected areas in Brazil: Evolution, land use and cover, and impact on emissions inventory. *Floresta* **2021**, *51*, 174–183. [CrossRef]
75. Sist, P.; Piponiot, C.; Kanashiro, M.; Pena-Claros, M.; Putz, F.E.; Schulze, M.; Verissimo, A.; Vidal, E. Sustainability of Brazilian forest concessions. *For. Ecol. Manag.* **2021**, *496*, 119440. [CrossRef]
76. Sheppard, J.P.; Chamberlain, J.; Agúndez, D.; Bhattacharya, P.; Chirwa, P.W.; Gontcharov, A.; Sagona, W.C.J.; Shen, H.-L.; Tadesse, W.; Mutke, S. Sustainable forest management beyond the timber-oriented status quo: Transitioning to co-production of timber and non-wood forest products—A global perspective. *Curr. For. Rep.* **2020**, *6*, 26–40. [CrossRef]
77. Klimas, C.M.; Cropper, W.P.; Kainer, K.A.; de Oliveira Wadt, L.H. Multimodel projections for evaluating sustainable timber and seed harvest of *Carapa guianensis*. *For. Sci.* **2018**, *61*, 15–27.
78. Vasconcelos, R.G.; Linhares, A.C.C.; Marques, M.B.L.; Alves, S.R.M. Análise da oferta de oleorresina de Copaíba (*Copaifera* spp.) no Brasil e do dinamismo do valor da produção. *Divers. J.* **2020**, *5*, 684–692. [CrossRef]